Dynamic model to predict the association between air quality, COVID-19 cases, and level of lockdown[☆]

Yara S. Tadano [a, *], Sanja Potgieter-Vermaak [b, c], Yslene R. Kachba [d], Daiane M.G. Chiroli [d], Luciana Casacio [e], Jéssica C. Santos-Silva [f], Camila A.B. Moreira [g], Vivian Machado [h], Thiago Antonini Alves [h], Hugo Siqueira [i], Ricardo H.M. Godoi [g]

[a] Department of Mathematics, Federal University of Technology - Parana (UTFPR), Ponta Grossa, Brazil
[b] Ecology & Environment Research Centre, Manchester Metropolitan University, Manchester, United Kingdom
[c] Molecular Science Institute, University of the Witwatersrand, Johannesburg, South Africa
[d] Department of Production Engineering, Federal University of Technology - Parana (UTFPR), Ponta Grossa, Brazil
[e] Center for Marine Studies, Federal University of Parana (UFPR), Pontal Do Paraná, Brazil
[f] Department of Water Resources and Environmental Engineering, Federal University of Parana (UFPR), Curitiba, Brazil
[g] Department of Environmental Engineering, Federal University of Parana (UFPR), Curitiba, Brazil
[h] Department of Mechanical Engineering, Federal University of Technology - Parana (UTFPR), Ponta Grossa, Brazil
[i] Department of Electric Engineering, Federal University of Technology - Parana (UTFPR), Ponta Grossa, Brazil

ARTICLE INFO

ABSTRACT

Studies have reported significant reductions in air pollutant levels due to the COVID-19 outbreak worldwide global lockdowns. Nevertheless, all of the reports are limited compared to data from the same period over the past few years, providing mainly an overview of past events, with no future predictions. Lockdown level can be directly related to the number of new COVID-19 cases, air pollution, and economic restriction. As lockdown status varies considerably across the globe, there is a window for mega-cities to determine the optimum lockdown flexibility. To that end, firstly, we employed four different Artificial Neural Networks (ANN) to examine the compatibility to the original levels of CO, O_3, NO_2, NO, $PM_{2.5}$, and PM_{10}, for São Paulo City, the current Pandemic epicenter in South America. After checking compatibility, we simulated four hypothetical scenarios: 10%, 30%, 70%, and 90% lockdown to predict air pollution levels. To our knowledge, ANN have not been applied to air pollution prediction by lockdown level. Using a limited database, the Multilayer Perceptron neural network has proven to be robust (with Mean Absolute Percentage Error ~ 30%), with acceptable predictive power to estimate air pollution changes. We illustrate that air pollutant levels can effectively be controlled and predicted when flexible lockdown measures are implemented. The models will be a useful tool for governments to manage the delicate balance among lockdown, number of COVID-19 cases, and air pollution.

© 2020 Elsevier Ltd. All rights reserved.

Artificial Neural Networks showed to be robust predictive tools to estimate the best equilibrium among COVID-19 cases, lockdown percentage, and air pollutants level.

1. Introduction

The World Health Organization (WHO) stated that South America is the new epicenter of the coronavirus pandemic (CNBC, 2020), and Brazil, one of the countries with the highest incidence of new cases and the second highest total number of cases in the world. A study done by scientists from Imperial College, London, showed that Brazil had the highest rate of transmission (R_0 of 2.81) among the 48 countries they investigated (The Lancet, 2020). To date (September 3, 2020), 6.6% of Brazil's total cases (3,997,865) were recorded in São Paulo city (262,570). This number constitutes more than 30% of the cases reported in São Paulo state (826,331). On September the 3rd the number of deaths in São Paulo city was 11,554 (4.4% of confirmed cases of COVID-19 led to death), higher than the global (3.3%) (SEADE, 2020).

Due to the rapid person-to-person transmission of COVID-19, São Paulo state government ordered lockdown on March 24, 2020, closing all (Secondary schools, Universities, Shopping Malls and, other commercial entities) but essential services (Nakada and Urban, 2020). As expected, beyond the efficiency to suppress the R_0 (Wilder-Smith and Freedman, 2020), these actions led to the scaling down in traffic, industrial and trade activities, and consequent reduction in air pollution levels, therefore improving air quality as a whole (Dutheil et al., 2020).

In response to the exponential increase in infection rates of the virus worldwide, local and national governments relaxed environmental legislation. For instance, the US EPA allowed industries and other facilities autonomy to decide and report if they meet the legislated requirements (Wu et al., 2020). Similarly, the Brazilian government has largely negated enforcement of environmental legislation during the coronavirus outbreak (The Guardian, 2020), which resulted in additional industrial air pollution emission, as well as, an increase in deforestation in the Amazon (de Oliveira et al., 2020). The danger is that reduced enforcement will continue past virus's peak to stimulate the economy and therefore put the population at risk.

Various scientists reported decreased air pollutant levels, comparing pre- and post COVID-19 air pollution levels using different methods and scales (Chauhan and Singh 2020; Dantas et al., 2020; Le et al., 2020; Li et al., 2020; Muhammad et al., 2020; Nakada and Urban, 2020; Sharma et al., 2020; Shehzad et al., 2020; Tobías et al., 2020). However, the available air pollution studies related to the COVID-19 situation are based on satellite images, air quality modeling and generally comparing lockdown period data with monthly means over the past few years. Worldwide, most studies reported in the literature indicated reductions in NO_x and $PM_{2.5}$ levels and an increase in O_3 concentration during lockdown (Nakada and Urban, 2020; Sharma et al., 2020; Sicard et al., 2020; Siciliano et al., 2020; Tobías et al., 2020). The following are a few examples of studies using these approaches.

Many researchers worldwide reported a reduction in NO_2 concentration levels (Chauhan and Singh, 2020; Muhammad et al., 2020; Zambrano-Monserrate et al., 2020). Zambrano-Monserrate et al. (2020) reported reductions in China, USA, Italy, and Spain, when Copernicus Atmosphere Monitoring Service data for $PM_{2.5}$ and NO_2 were compared to the previous three years. Rodríguez-Urrego and Rodríguez-Urrego (2020) studied $PM_{2.5}$ profiles of the 50 most polluted countries and reported an average reduction of 12% worldwide. They used the World Air Quality Index platform to obtain data and compared it to the previous 2 years.

Closer to home, Dantas et al. (2020) and Nakada and Urban (2020) compared various air pollutants (including CO, O_3, NO_2, NO, $PM_{2.5}$, PM_{10}, and SO_2) over different time scales (one year to five-year trend) in Rio de Janeiro and São Paulo, respectively. In both cases, local data were used. Both studies indicated a reduction of all pollutants investigated, except for ozone, which increased.

These approaches (using satellite images, air quality modeling and generally comparing lockdown period data with monthly means over the past few years) are limited as it provides mainly an overview of past events, with no future predictions.

Artificial Neural Networks (ANN), on the other hand, is a nonlinear methodology capable of mapping a set of inputs into an output, which is important to support decisions regarding preventive measures. This approach has been used in air pollution epidemiological studies (Araujo et al., 2020; Kachba et al., 2020; Kassomenos et al., 2011; Tadano et al., 2016; Polezer et al., 2018). In Araujo et al. (2020) and Kassomenos et al. (2011), the ANN showed a better performance than linear approaches as Generalized Linear Models. Kassomenos et al. (2011) also concluded that ANN is a more flexible and adaptive mathematical approach.

In this context, as lockdown status varies considerably across the globe, there is a window of opportunity for mega-cities to determine the optimum level of lockdown to ensure effective management of transmission rates, air quality, and a healthy economy. To our knowledge, ANN have not been applied to air pollution prediction by lockdown level.

To that end, we used four Artificial Neural Networks (ANN) (Extreme Learning Machine − ELM; Echo State Network − ESN; Multilayer perceptron − MLP and Radial Basis Function Networks − RBF) to estimate the influence that newly reported COVID-19 cases and lockdown level may have on the local air pollution (CO, O_3, NO_2, NO, $PM_{2.5}$, and PM_{10} levels) in São Paulo city. After checking compatibility, we simulated four hypothetical partial lockdown scenarios (10, 30, 70, and 90%) to investigate the relationship between reduced activities and air quality.

In the light of evidence that poor air quality may exacerbate COVID-19 symptoms (Wu et al., 2020), and potentially lead to higher mortality rates, the ANN showed to be a useful predictive tool for governments. Using this approach, resumption of industrial and other activities can be managed to ensure a sustainable balance among economic health, air quality, and transmission rate.

2. Materials and methods

The data of São Paulo city was selected to examine the robustness of our approach. São Paulo is the most populous city of Latin America, with around 12.25 million inhabitants (IBGE, 2020), the main hotspot of COVID-19 in Brazil, and one of the most polluted cities in Latin America. The inputs were: daily number of COVID-19 cases, partial lockdown level, and meteorological variables; the outputs were the daily concentration of each air pollutant (CO [ppm], O_3 [μg/m^3], NO_2 [μg/m^3], NO [μg/m^3], $PM_{2.5}$ [μg/m^3], and PM_{10} [μg/m^3]).

Data on the daily number of newly reported COVID-19 cases and lockdown percentages was collected from March 17, 2020 to May 13, 2020 from the Statistical Portal of São Paulo State (SEADE, 2020). The Intelligence Monitoring System of São Paulo has an agreement with mobile phone companies to track people's movement. This georeferenced anonymised information is available on the SEADE website and has been used in this study.

Meteorological variables were extracted from the Environmental Company of São Paulo State database (CETESB). These included: relative humidity − RH [%]; maximum temperature − MT [^{o}C]; atmospheric pressure − AP [hPA]; wind speed − WS [m/s] and global solar radiation−GSR [W/m^2]) (CETESB, 2020).

The data on target pollutant levels of CO [ppm], O_3 [μg/m^3], NO_2 [μg/m^3], NO [μg/m^3], $PM_{2.5}$ [μg/m^3], and PM_{10} [μg/m^3] concentrations were selected from January 01, 2020 to May 13, 2020 (134 samples). As a matter of comparison and to improve the ANN performance, we included the data for a period with zero COVID-19 cases and no lockdown (data from January 01, 2020 to March 16, 2020).

Daily concentrations were extracted from the CETESB. More than sixty-six percent of the hourly averages were similar to the daily average. The data were ratified by the CETESB, who follows the quality assurance/quality control (QA/QC) procedure approved by the State Council of Environment (CONSEMA) of the State of São Paulo. Beta radiation is used for PM_{10} and $PM_{2.5}$ measurements, chemiluminescence for NO_2 and NO, non-dispersive infrared for CO, and ultraviolet analysis for O_3 (CETESB, 2020).

Data from four CETESB air quality monitoring stations (AQMS) were used due to their locations (Fig. 1). The largest data sets could be obtained from D. Pedro II station (blue spot - located in a high

Fig. 1. Locations of the air quality monitoring stations in São Paulo. The satellite map is from Google Maps (Map data©2020 Google; https://www.google.com/maps/place/Brazil/); the satellite is from Google Earth Pro (Map data©2020 Google; www.google.com/maps/@-23.6815315,-46.8754814,10z). The maps were edited with Microsoft Power Point (version 16.28−19081202). Note: AQMS: Air Quality Monitoring Station; Tietê: ring road; D. Pedro II: downtown; *Tietê station has no O3 data and was replaced by data from USP-Ipen station.

demographic density area) and Tietê station (red spot located near a busy ring road). D. Pedro II station is located downtown − high demographic density area; influenced mainly by a light-duty fleet, and Tietê station is near a ring road, characterized mainly by heavy-duty emissions.

Table 1 shows that even at these two stations, some data is lacking. PM$_{2.5}$ data from D. Pedro II station had several gaps in the data set for consecutive days, and these were replaced by data from Mooca station (yellow spot) (CETESB, 2020), as the linear correlation of the data with those from D. Pedro II station is 0.95. For missing data from non-consecutive days, the previous day's values were used. Tietê station had no ozone data, and it was supplemented by data from a nearby location USP-Ipen station (green spot).

2.1. Artificial Neural Networks

The four ANN used in this study are described below (further details in Araujo et al. (2020)).

2.1.1. Multilayer Perceptron overview

The Multilayer Perceptron (MLP) is a neural model able to map any nonlinear, continuous, limited, and differentiable function with arbitrary precision, which confers a characteristic of a universal approximator (Haykin, 2008). The basic structure of an ANN is the

Table 1
Number of days with no data for each studied AQMS.

AQMS	CO	O$_3$	NO$_2$	NO	PM$_{10}$	PM$_{2.5}$
Tietê*	2	0*	0	0	1	2
D. Pedro II	4	1	0	0	0	10

Note: AQMS: Air Quality Monitoring Station; Tietê: ring road; D. Pedro II: downtown; * Tietê station has no O3 data and was replaced by data from USP-Ipen station.

artificial neurons, functional units responsible for processing the information, and providing the output response (de Castro, 2007).

In an MLP, the neurons are distributed in three kinds of layers. The input layer transmits the data to the intermediate (hidden) layers, where the neurons perform a nonlinear transformation, mapping the input signal to another space. Then, the signal is sent to the output layer, in which the output signal is generated based on a linear combination, in most cases. Neurons from the same layer are disconnected, while those from disjoint layers fully exchange information since this is a feed forward model (Siqueira and Luna, 2019).

Training a neural model means using an algorithm to determine its free parameters or adjust the neurons' weights. The most known way to solve this task in an MLP is to use the backpropagation algorithm, a general iterative tool based on the steepest descent, a first order unrestricted linear optimization method. In this case, the method reduces the mean square error between the desired response and the output of the network (Haykin, 2008). However, in this work, we address a second-order method that presents computational cost similar to the first: The Modified Scaled Conjugate Gradient (MSCG) (dos Santos and Von Zuben, 1999).

We highlight the maximum number of iterations as the stop criterion in training. We also use the hold-out cross-validation method to determine the topology (number of neurons in the hidden layer) and avoid overfitting (Haykin, 2008).

2.1.2. Radial basis function

The Radial Basis Function networks (RBF) are a well-known ANN model. Like the MLP, they are feed forward architectures, and universal approximators, but present only two layers of neurons (Siqueira and Luna, 2019). The first, intermediate, perform a nonlinear input-output mapping using radial basis functions, like the Gaussian function. The second − output layer −performs the model's response, similarly to the MLP (Haykin, 2008).

The hidden neurons present two parameters: a centre c_i (with

the same dimension of the number of inputs), and a dispersion σ_i Therefore, the output of each neuron is higher to inputs that are spatially closer to the current centre. The dispersion is responsible for modulating the decay of the response concerning the distance between the inputs and the centers. Usually, the Gaussian function is addressed as RBF. A linear combinator is used to perform the output response (Siqueira and Luna, 2019).

The training process of an RBF is performed in two steps. The first is the adjustment of the hidden neurons (centers and dispersions), a task performed by the unsupervised clustering method. In this work, we addressed the K-Medoids algorithm. Also, we assumed that all dispersions are the same (Haykin, 2008). The second step is the adjustment of the output neurons. A simple and efficient tool found in the literature is the use of the Moore−Penrose inverse operator (Haykin, 2008).

2.1.3. Extreme Learning Machines

Extreme Learning Machines (ELM) are feed forward neural models, with a single hidden layer (Huang et al., 2006, 2015). This structure is quite similar to the classic MLP, the training process being the main difference (Siqueira et al., 2018).

In an ELM, the intermediate neurons have weights randomly generated, and they are not adjusted during the running time. The insertion of new neurons in the hidden layer leads to a decrease in the output error (Siqueira et al., 2012a).

Then, an ELM training is summarized in finding the best set of weights of the output layer. The main manner to overcome this task is to use a minimum square solution, especially the Moore−Penrose generalized inverse operation (Siqueira et al., 2018).

2.1.4. Echo State Networks

The Echo State Networks (ESN) are architectures of ANN, which present high similarity with the ELM, regarding the structure and training process. However, unlike the previously mentioned networks, this is a recurrent model since it presents feedback loops of information. In this case, the hidden layer, named dynamic reservoir, has such recurrence (Jaeger, 2001, 2002).

Jaeger (2001, 2002) demonstrated that the reservoir is a nonlinear transformation, which is influenced by the recent samples of the input signal, so that we can choose the weights in advance if specific conditions are respected. In this work, we used the reservoir design by (Jaeger, 2001).

As in the ELM, the training is responsible for determining the weights of the output layer, which may be done using the Moore−Penrose generalized inverse operation, as in the ELM case (Siqueira et al., 2018).

2.2. Computational details

The computational step involved the seven input variables mentioned above: number of COVID-19 new cases, partial lockdown level, maximum temperature, relative humidity, atmospheric pressure, wind speed, and global solar radiation. The desired signals (target) were each air pollutant's (CO, O_3, NO_2, NO, $PM_{2.5}$, and PM_{10}) concentration.

We evaluated the performance considering all the inputs at the same time; without the number of new COVID-19 cases; and without the number of new COVID-19 cases and partial lockdown, to analyze the robustness of the neural networks on predicting air quality according to COVID-19 variables and using a small database. All cases included the meteorological variables.

To perform the computational analysis, we separated the dataset in three subsets:

- Training: from January 01 to April 23, 2020 (114 samples);

- Validation: April 24 to May 03, 2020 (10 samples);
- Test: May 04 to May 13, 2020 (10 samples).

The training subset is used to adjust the models, and the validation is applied to verify the overtraining and define the number of neurons in the intermediate layer. Finally, the test subset is used to evaluate the performance of the models. We also verified if the use of the Z-score may bring some performance gain. It is a mathematical treatment that transforms the series of data into approximately stationary. Some studies have presented the importance of using such an approach (Kachba et al., 2020; Siqueira et al., 2018).

To apply the Z-score, the value of each sample is subtracted from the mean and divided by the standard deviation. At the end of the ANN execution, the process is reversed to analyze the performances in the original domain.

The number of neurons in the hidden layer was defined by empirical tests, varying from 3 to 100 neurons. The best number for each case was chosen based on the lower Mean Square Error (MSE) in the test set. The number of neurons in the hidden layer of each neural model is in Tables A1 and A2 in Appendix A.

We followed the premises from the literature of adopting the MSE as the most important error metric because this is reduced during the training (adjustment) of the neural models (Araujo et al., 2020; Kachba et al., 2020; Siqueira et al., 2014, 2018, 2020).

The artificial neurons in the intermediate layer of the MLP, ELM, and ESN, use the hyperbolic tangent as an activation function. In the RBF, the Gaussian function is used. The MLP training addressing the Modified Scaled Conjugate Gradient (MSCG) and uses as stop criterion the maximum number of 500 iterations. Also, the K-Medoids in RBF achieved the stop criterion after 10 iterations without modification in the position of the centroids (Figueiredo et al., 2019).

3. Results and discussion

For simplicity, we divided this section into three parts. Firstly, the descriptive analysis of the databases, followed by the ANN prediction results, and lastly, the results for the hypothetical scenarios of 10%, 30%, 70%, and 90% of lockdown.

3.1. Descriptive analysis

The daily concentrations during the studied period, together with the partial lockdown level, are shown in Appendix A - Figure A1. The São Paulo state government officially ordered lockdown on March 24, 2020, however, the population started to self-isolate voluntarily the week before (first available social isolation data − March 17, 2020). From March 17, 2020 to May 13, 2020, the lockdown varied between 38 and 59%, with an average of 51%.

To visualize changes in air pollution levels due to voluntary self-isolation and/or lockdown, we compared the five-day average before (12−16 March 2020) voluntary self-isolation with a five-day average during self-isolation (17−21 March 2020) (Fig. 2). There is no distinctive change in pollutant levels within experimental error, as may be expected due to a lag in response and a low level of reduced activities. However, comparing a five-day average during the first lockdown period (54−56% lockdown from 24 to 28 of March 2020) with the period before lockdown or self-isolation, we do observe a general decrease in pollutant levels for all pollutants at Tietê and for most at D. Pedro II as is shown in Fig. 3. As this period would reflect the changes in the self-isolation period's activities with additional reduction of activities, this finding is not surprising. From Figure A1 we observe that this trend continues until
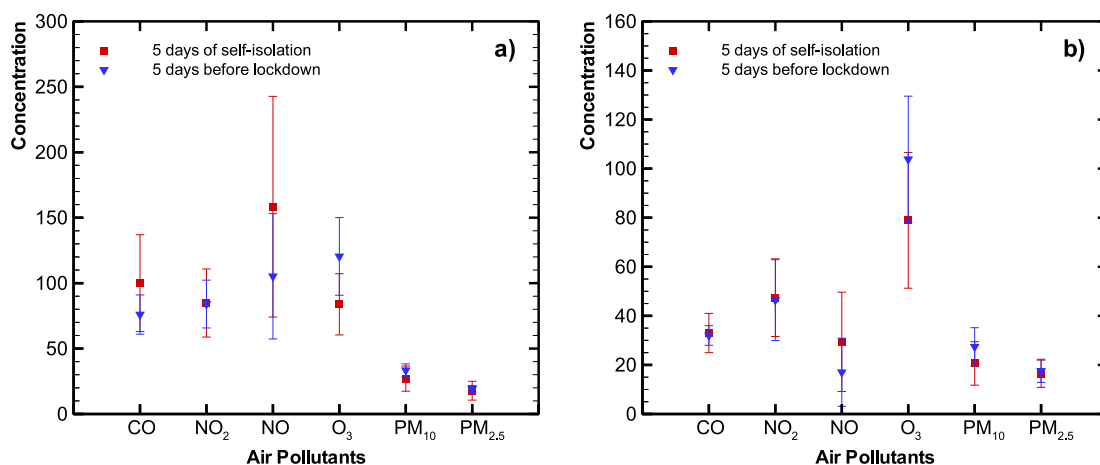
Fig. 2. Five-day average pollutant levels before and during the voluntary self-isolation period at Tietê station (a) and D. Pedro II station (b) (CO concentration were multiplied by 100).
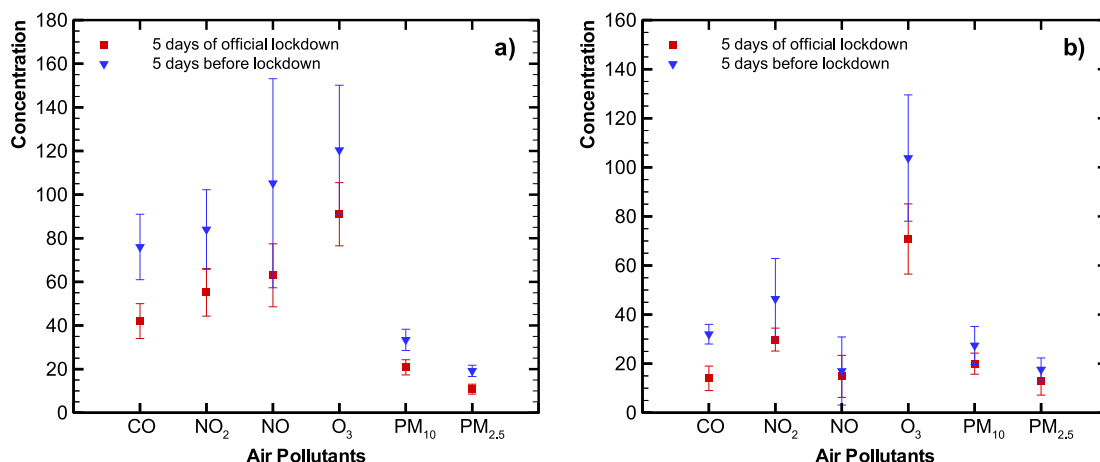

Fig. 3. Averages comparison between five days of official lockdown with five days before lockdown for Tietê station (a) and D. Pedro II station (b) (CO concentration were multiplied by 100).

around the 24th of April, after which relaxation in lockdown rules corresponds to a steady increase in most of the pollutant levels. It does seem as though not all the pollutants are similarly influenced by the lockdown. The particulate matter concentration appears to be influenced by other factors as well, and reaches much higher values towards the end of the lockdown period discussed here than what it was before. The ozone levels generally increased with a lockdown percentage increase.

Using a neural network to study atmospheric ozone formation in the Metropolitan Area of São Paulo (MASP), Guardani et al. (1999) found that temperature was the main factor affecting ozone formation and observed higher ozone levels in regions characterized by lower emission levels of ozone precursors. Martins and Andrade (2008) evaluated VOC s' potential for ozone formation using a three-dimensional air quality model and found that ozone in the MASP is VOC-limited, as commonly observed in urban areas (Li et al., 2019; Siciliano et al., 2020; Tobías et al., 2020). Under these conditions, a decrease of NO_x can reduce the removal of O_3 through NO_x titration and/or the effect of radical terminating reactions, and thereby increasing O_3 formation (Seinfeld and Pandis, 2016; Sillman, 1999, 2003). Furthermore, Andrade et al. (2017), studying the MASP, explain that decreasing NO_x and CO emissions simultaneously contribute to higher ozone levels. This behavior is also affirmed in (Gentner et al., 2009; Harley et al., 2005; Marr and Harley, 2002; Stedman, 2004).

Table 2 presents the linear correlations between the lockdown level (varying from 38 to 59%) and air pollutant concentrations at Tietê and D. Pedro II stations for March 17, 2020 (first day of available data of social isolation) to May 13, 2020. Bar ozone, all the pollutants correlated negatively (ranging from −0.14 for CO at D. Pedro II to −0.60 for NO at Tietê) with the lockdown.

Finally, Appendix A - Figure A2 shows the number of daily COVID-19 newly reported cases. The first day of registered COVID-19 cases was February 25, 2020 and an exponential increase is observed from the beginning of April onwards.

Table 2
Linear correlations between lockdown and studied air pollutant concentrations for March 17, 2020 to May 13, 2020.

	CO	O_3*	NO_2	NO	PM_{10}	$PM_{2.5}$
Tietê	−0.45	0.15	−0.57	−0.60	−0.34	−0.38
D. Pedro II	−0.14	0.11	−0.42	−0.33	−0.23	−0.26

Note: *Data from USP-Ipen station.

Table 3
Average and standard deviation for each studied pollutant for the 3 subsets (Tietê Station).

Pollutant	Training		Validation		Test	
	Average	Standard Deviation	Average	Standard Deviation	Average	Standard Deviation
CO [ppm]	0.69	0.29	0.93	0.46	0.85	0.34
O_3 [μg/m^3]	70	28	98	21	74	14
NO_2 [μg/m^3]	68	24	86	31	88	31
NO [μg/m^3]	91	69	124	89	151	84
$PM_{2.5}$ [μg/m^3]	13	5.5	24	12	20	9.7
PM_{10} [μg/m^3]	22	8.2	43	19	38	19

Table 4
Average and standard deviation for each studied pollutant for the 3 subsets (D. Pedro II Station).

Pollutant	Training		Validation		Test	
	Average	Standard Deviation	Average	Standard Deviation	Average	Standard Deviation
CO [ppm]	0.30	0.15	0.62	0.40	0.50	0.36
O_3 [μg/m^3]	65	24	81	19	59	14
NO_2 [μg/m^3]	43	17	60	33	64	31
NO [μg/m^3]	21	19	51	63	75	76
$PM_{2.5}$ [μg/m^3]	12	4.7	20	8.8	16	7.8
PM_{10} [μg/m^3]	19	7.3	37	14	31	16

3.2. ANN estimation analysis

Tables 3 and 4 contain the average and standard deviation for each pollutant level obtained from the 3 subsets (training, validation, and test) at the two sites. Although the two monitoring sites are in the same city, the descriptive statistics show significant differences. Tietê station (near highways) has higher average concentrations for all pollutants in comparison to D. Pedro II station (populated city area). The different statistical profiles of the two sites are indicative of robust evaluation of the data, as the model could provide a MAPE of ~30%, despite two dissimilar data sets.

Tables A1 and A2 (Appendix A) display the ANN computational results for AQMS Tietê (ring road station) and AQMS D. Pedro II (densely populated city area station), respectively. For this purpose, the best (lower Mean Square Error - MSE) of 30 independent executions were considered (de Castro, 2007; Haykin, 2008; Siqueira et al., 2018). The shaded values indicate results with the best performance (lower MSE). The MLP neural model achieved the best results (i.e., lowest MSE) in almost all cases, except for O_3 at D. Pedro II station. The latter was best estimated using the ELM neural model. It is an important observation, as there is no consensus about which ANN is the best. It corroborates with the results achieved by Polezer et al. (2018) and Araujo et al. (2020), both applied to air pollution epidemiological studies.

It is important to highlight that the best overall ANN results were achieved when the variables "number of new COVID-19 cases" and "partial lockdown" were included (8 out of 12 cases). The remaining 4 cases (NO_2 and $PM_{2.5}$ at Tietê, and NO_2 and O_3 at D. Pedro II) showed the best result considering only "partial lockdown". In both scenarios the meteorological variables were included.

To establish if the Z-Score application could result in performance gain, the ANN was also performed with the Z-score (Results shown in Tables A1 and A2). The Z-score's use proved to be beneficial in 2 cases at the Marginal Tietê station, and four cases at the D. Pedro II site. Therefore, it can be considered in addition to increasing the quality of the results of the ANN.

Figs. 4 and 5 represent the observed (continuous red line) and best estimation (dashed blue line) concentration levels for CO (a), O_3 (b), NO_2 (c), NO (d), $PM_{2.5}$ (e), and PM_{10} (f) at Tietê and D. Pedro II stations, respectively during the period 4–13 May 2020. The lockdown level is indicated as shaded bars.

In general, the predicted results, using this approach, captured the original data tendencies reasonably well, with a mean absolute percentage error (MAPE) of 30% for almost all cases. The exceptions were at D. Pedro II station (CO − 48% and NO - 81%) (see Tables A1 and A2 − Appendix A).

It is important to notice two distinct behaviors during the lockdown to the test set period (see Figs. 4 and 5). When the lockdown level remains unchanged (first 5 days), the main influence can be ascribed to the meteorological variables (Figure A3 − shows the meteorological raw data for the test period). But after five days in the test set, the percentage lockdown jumps from 46% to 53% in two days. As the temperature and relative humidity were relatively stable in the last five days, one can say that the lockdown is the main contributor to the change in air pollutant level. Observe that ozone concentration has a consistent relation with solar irradiation, with similar profiles. This behavior is in accordance with those observed at the beginning of lockdown (March 17, 2020), as mentioned in section 3.1. The importance of maintaining continuous and consistent interventions to curb air pollution is evident from the data displayed here. It is particularly important during extreme air pollution events, and there is enough evidence that lockdown measures will nearly instantly reduce air pollution levels.

Each ANN architecture has positive and negative points. As discussed in Section 2.1, the ESN is a recurrent model, presenting feedback loops of information in its hidden layer. This characteristic may be relevant when dealing with data processing since more information is available to form the output response. Additionally, together with the ELM, their training processes require less computational effort than the RBF and MLP, since there are no iterative processes to adjust their weights because the hidden layer is not modified. In addition, other works have presented the capability of such models to overcome traditional, fully trained architectures (Araujo et al., 2020; Siqueira et al., 2012a, 2014, 2018).

Despite the advantage and good results found in the literature for ESN, ELM, and RBF (Siqueira et al., 2012b, 2018), the MLP errors were smaller than the others. It seems clear that adjusting the hidden weights is an important step in nonlinear mapping applications, as is presented in this investigation. In this case, there are a set of inputs of variable nature (for example, temperature, humidity, and partial lockdown), and mapping these values to another
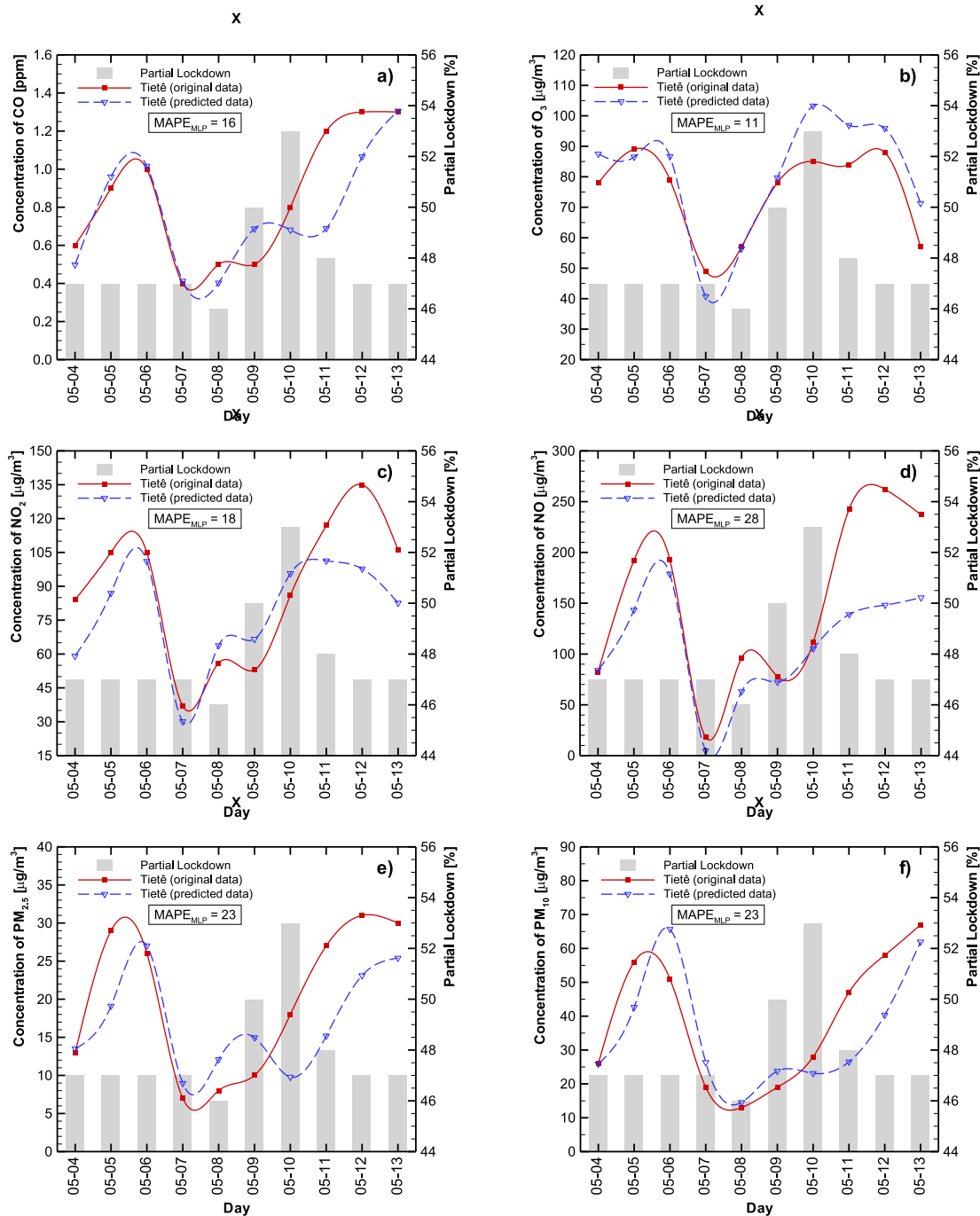
Fig. 4. Best estimation to predict CO (a), O_3 (b), NO_2 (c), NO (d), $PM_{2.5}$ (e), and PM_{10} (f) levels for Tietê station. Predictions are in dashed lines and observed levels in solid lines. The bars are the partial lockdown.
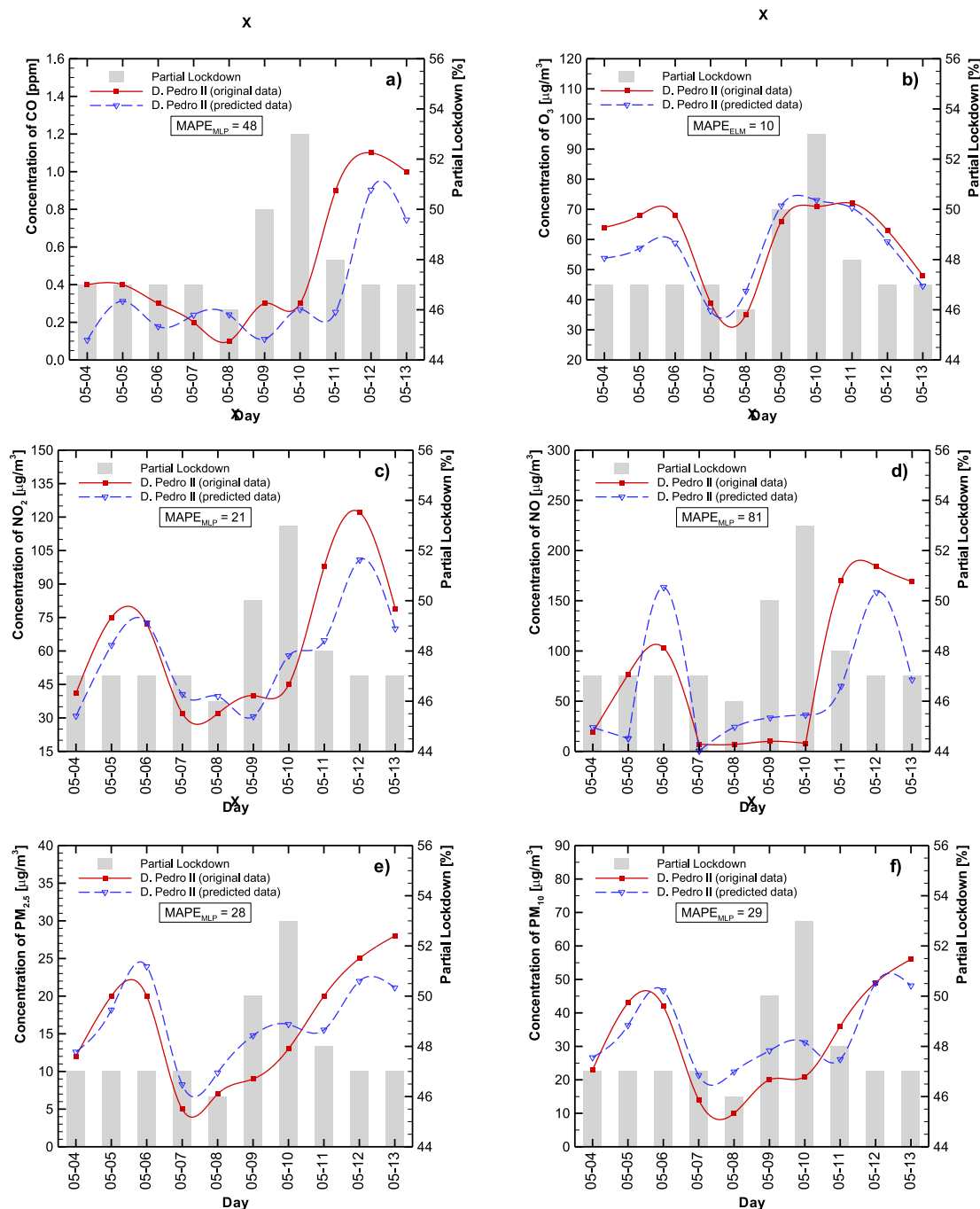
Fig. 5. Best estimation to predict CO (a), O_3 (b), NO_2 (c), NO (d), $PM_{2.5}$ (e), and PM_{10} (f) levels for D. Pedro II station. Predictions are in dashed lines and observed levels in solid lines. The bars are the partial lockdown.
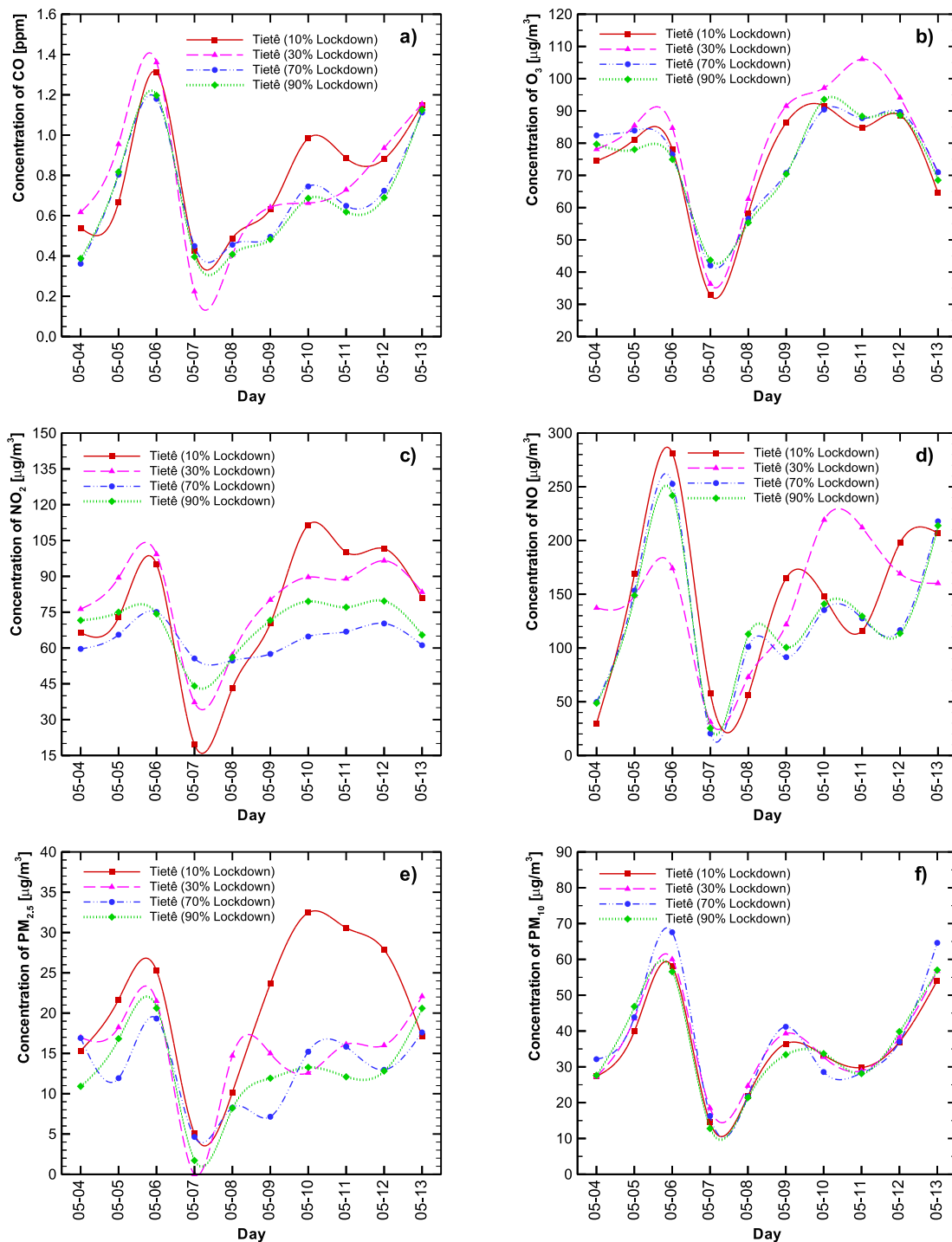
Fig. 6. Hypothetical scenarios considering the impact that 10% (red line), 30% (pink like), 70% (blue line), and 90% (green line) lockdown would have on CO (a), O_3 (b), NO_2 (c), NO (d), $PM_{2.5}$ (e), and PM_{10} (f) levels for AQMS Tietê. (For interpretation of the references to colour in this figure legend, the reader is referred to the Web version of this article.)
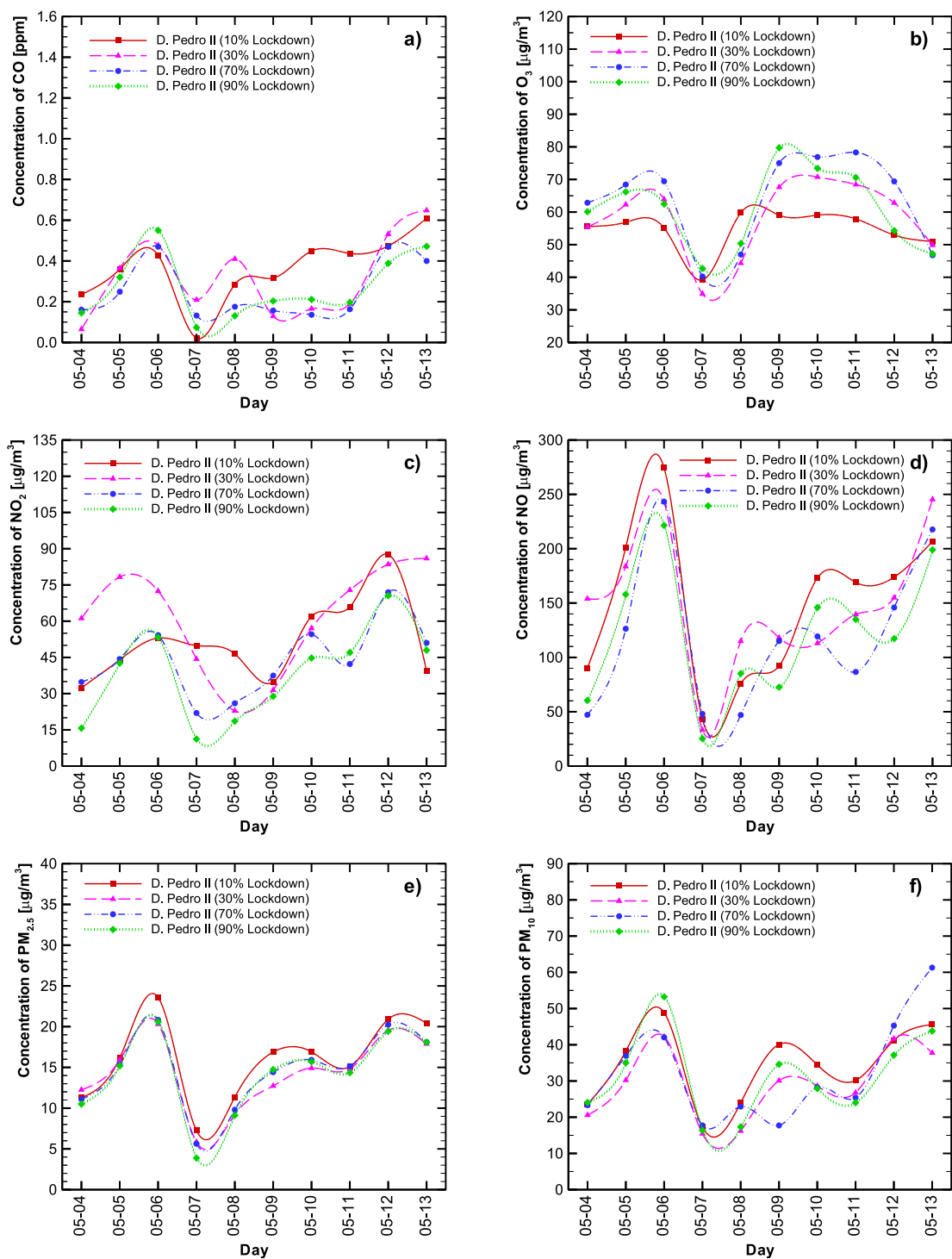
Fig. 7. Hypothetical scenarios considering the impact that 10% (red line), 30% (pink like), 70% (blue line), and 90% (green line) lockdown would have on CO (a), O_3 (b), NO_2 (c), NO (d), $PM_{2.5}$ (e), and PM_{10} (f) levels for AQMS D. Pedro II. (For interpretation of the references to colour in this figure legend, the reader is referred to the Web version of this article.)

variable is not a trivial task (Kachba et al., 2020; Polezer et al., 2018).

3.3. Hypothetical scenarios

To predict the impact that the partial lockdown has on air quality, four hypothetical scenarios were modeled: a minimum lockdown level (10%); possible vertical isolation (only for COVID-19 high-risk groups — over-60s and people with chronic disease, diabetics, among others) (30%); the considered ideal lockdown percentage (70%); and an extreme isolation action (90%). The results are compared in Figs. 6 and 7, with results for AQMS Tietê D. Pedro II, respectively. The red lines correspond to 10% lockdown, the pink lines to 30% lockdown, the blue lines to 70% lockdown, and the green lines to 90% lockdown. The pollutant designation (a -f) is the same as for Figs. 4 and 5.

The data in Fig. 6 (Tietê station) indicates that in general higher concentrations are predicted for all pollutants at 10 (red line) and 30 (pink line) % lockdown. A different pattern is observed for May 07 and May 08, whereby the lower lockdown also predicted low pollutant concentrations. During these two days, the meteorological conditions changed abruptly (low temperature and solar irradiation, and high relative humidity - see Figure A3). This scenario exemplifies the complex interdependency of air pollutant levels on several variables. These findings suggest that when abrupt weather conditions are forecasted, lockdown interventions should happen a few days earlier. Our data corroborate with the recent publication of Hong et al. (2019) who reported that extreme weather events might be a crucial mechanism by which air quality is influenced.

The predicted ozone concentration at Tietê station (Fig. 6b) for the 30% lockdown showed an unexpected behavior, presenting higher concentrations than 70% and 90% lockdown. It may have been a consequence of the complexity of the variables that influence air quality. Although this may be seen as a poor fit for the model, we need to emphasize that this is one case out of twelve.

Although the same abrupt change in meteorological conditions was observed for 7 and 8 May at the D. Pedro II station (Fig. 7), the ANN could estimate the response more coherently than for the Tietê station. This may be due to other factors at play, influencing the air pollutant level at this station. Observe that the ozone profiles are as expected, especially for a 10% lockdown. It is important to highlight that the ANN prediction was good as only one of the seven inputs were changed.

We also observe that the particulate matter levels are not greatly influenced by lockdown (as reported by Nakada and Urban, 2020), especially the PM_{10} concentration. At the D. Pedro II station, the $PM_{2.5}$ levels also stay very similar regardless of the lockdown level.

We acknowledge that air pollutant levels have a complex set of variables that determine it, and that even a powerful tool such as ANN cannot always accurately predict the level. However, the data presented here provides adequate evidence that ANN can be used successfully to estimate the impact of different levels of lockdown will have on the air quality.

4. Conclusion

Artificial Neural Networks were able to predict how changes in the level of lockdown affected air quality in São Paulo City. We have shown that even when using a restricted data set of pollutant levels together with meteorological information, the ANN results showed Mean Absolute Percentage Error (MAPE) around 30%.

The result of the ANN approach to four hypothetical scenarios of lockdown (i.e., 10%, 30%, 70%, and 90%) showed evidence of the complexity of the calculation problem as a consequence of the abrupt meteorological changes.

For the first time, ANN were used as a tool to describe the equilibrium between air pollution, COVID-19 cases, and the partial lockdown, which can be employed in several national contexts. This approach's predictive power allows governmental bodies and policy makers to manage lockdown responsibly ensuring minimal economic impact. This method will lead to improved air pollution control measures (and potentially COVID-19 mortality) by enforcing a lockdown level that will still sustain sufficient economic activities. Furthermore, in the light of the global drive to improve air quality and work towards zero emissions, this approach could also be used in the future to reach emission target levels.

CRediT author statement

Yara S. Tadano, Conceptualization, Methodology, Data curation, Investigation, Validation, Formal analysis, Writing - original draft, Writing - review & editing. Sanja Potgieter-Vermaak: Writing - review & editing. Yslene R. Kachba, Conceptualization, Data curation. Daiane M.G. Chiroli, Writing - original draft. Luciana Casacio, Writing - review & editing. Jéssica C. Santos-Silva, Data curation, Writing - original draft. Camila A.B. Moreira, Data curation, Investigation. Vivian Machado, Visualization, Validation. Thiago Antonini Alves, Data curation, Visualization, Writing - original draft. Hugo Siqueira, Conceptualization, Methodology Software, Investigation, Validation, Formal analysis, Writing — original draf. Ricardo H.M. Godoi, Formal analysis, Writing — review.

Declaration of competing interest

The authors declare that they have no known competing financial interests or personal relationships that could have appeared to influence the work reported in this paper.

Acknowledgement

APPENDIX A

Figure A1 shows the behavior of each target (air pollutant concentration) before any modeling. A black line was included on the first day of partial lockdown available data (March 17, 2020). The shaded bars are the lockdown daily levels.
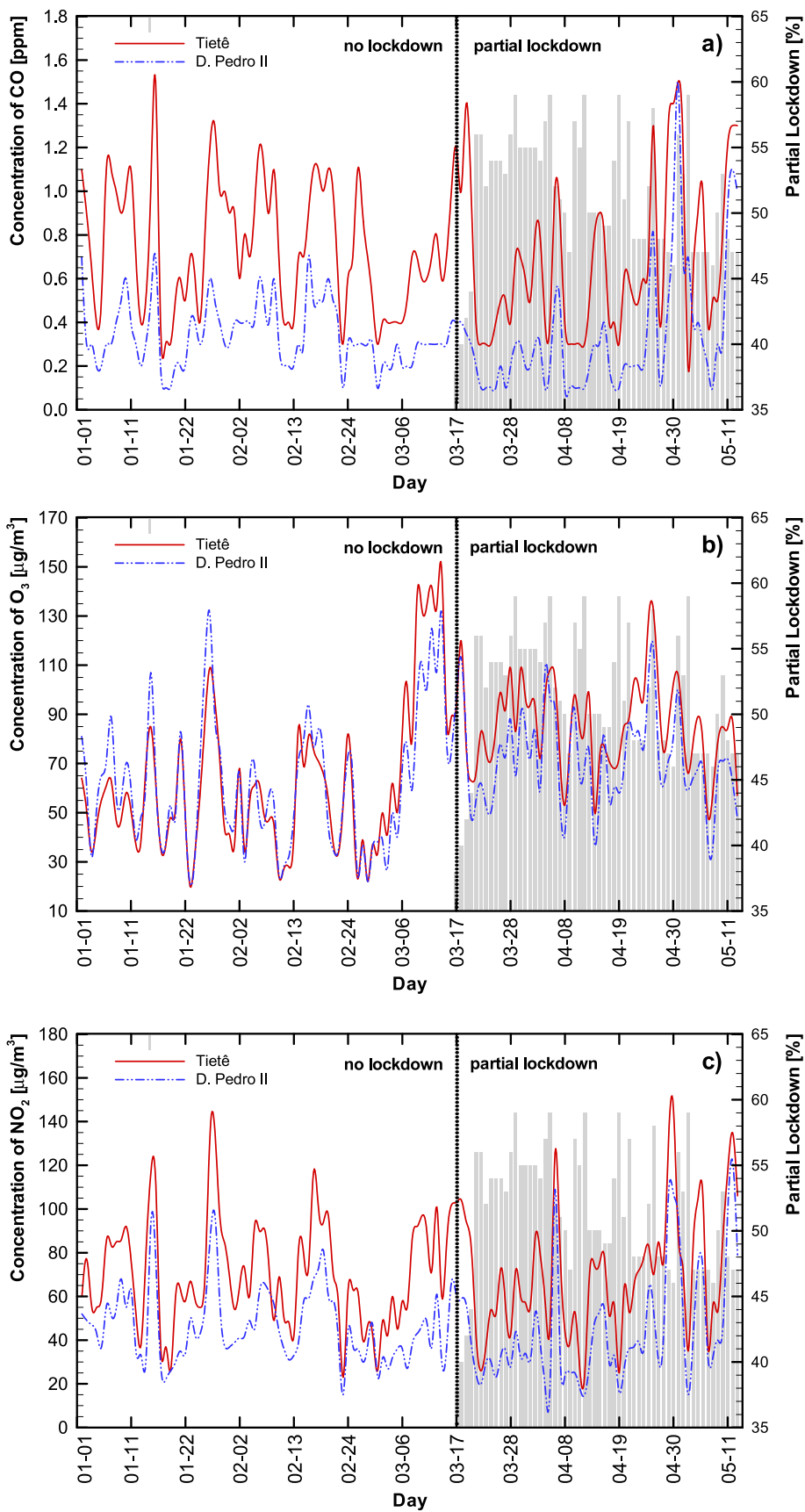
Fig. A1. Concentrations of CO [ppm] (a), O_3 [μg/m³] (b), NO_2 [μg/m³] (c), NO [μg/m³] (d), $PM_{2.5}$ [μg/m³] (e), and PM_{10} [μg/m³] (f) according to the date.
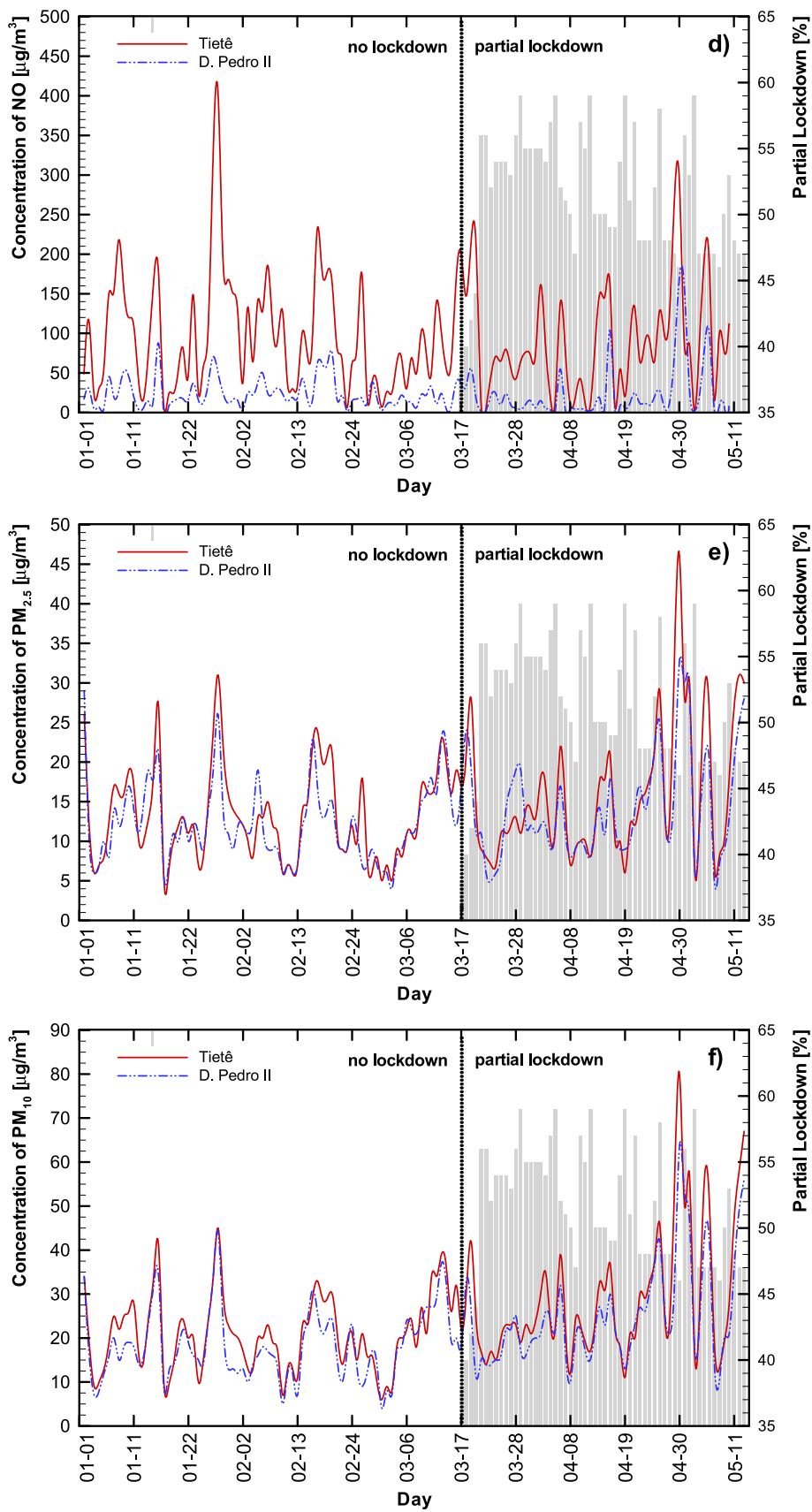
Fig. A1. (*continued*).
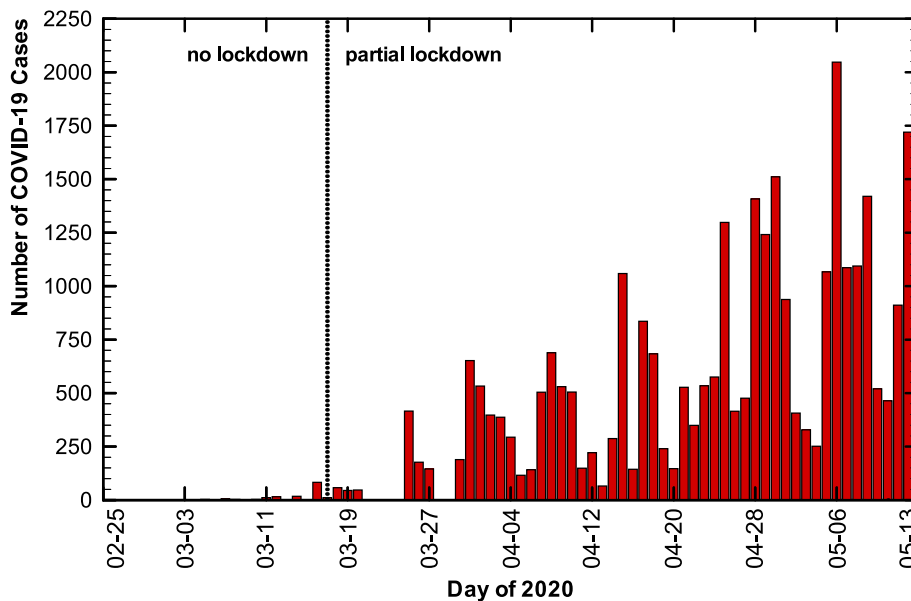
Fig. A2. Number of COVID-19 new cases by day.

Tables A1 and A2 show the ANN computational results at the AQMS Tietê (ring road station) and AQMS D. Pedro II (downtown station), respectively. The addressed scenarios involves the errors based on the Mean Square Error (MSE); Mean Absolute Error (MAE); and Mean Absolute Percentage Error (MAPE); with all inputs, without the number of COVID-19 new cases (without COVID), and also without the number of COVID-19 new cases and the partial lockdown (without COVID and lockdown). Also, the results considering or not the use of Z-Score are presented. The shade of gray values are the results showing the best performances (lower MSE).

Table A1
Computational results for Tietê Station

			CO				PM$_{10}$				PM$_{2.5}$			
			NN	MSE	MAE	MAPE	NN	MSE	MAE	MAPE	NN	MSE	MAE	MAPE
Without Z-Score	All Inputs	ELM	3	0.082	0.241	27.336	55	302.983	14.792	41.053	40	118.040	9.379	68.917
		ESN	3	0.104	0.275	35.007	10	226.953	12.543	36.529	70	84.089	8.198	60.844
		MLP	5	0.056	0.189	21.054	**35**	**125.516**	**89.970**	**22.795**	7	58.597	6.129	32.043
		RBF	90	0.107	0.290	41.937	90	361.600	17.400	71.145	7	116.624	8.700	82.812
	Without COVID	ELM	3	0.074	0.229	29.136	25	363.393	16.372	47.747	25	121.795	9.633	71.572
		ESN	3	0.068	0.227	29.313	17	355.852	16.807	55.639	17	73.759	7.760	54.564
		MLP	7	0.054	0.189	20.939	3	228.692	12.619	32.008	5	54.020	5.728	25.911
		RBF	90	0.107	0.290	41.912	90	361.758	17.414	71.173	90	116.684	8.708	82.843
	Without COVID and Lockdown	ELM	15	0.196	0.355	41.284	20	441.157	18.462	59.690	80	142.555	10.548	76.858
		ESN	5	0.072	0.216	24.928	30	447.592	19.187	62.825	60	124.008	9.233	68.624
		MLP	5	0.106	0.248	24.881	5	274.828	12.145	29.001	50	73.181	5.655	22.787
		RBF	90	0.107	0.291	42.002	90	361.429	17.544	71.302	90	116.337	8.720	82.882
With Z-Score	All Inputs	ELM	20	0.139	0.334	37.919	50	332.813	16.294	55.894	45	98.053	8.778	59.417
		ESN	3	0.090	0.243	27.409	20	274.429	13.738	54.822	35	110.166	8.710	67.406
		MLP	5	**0.039**	**0.135**	**16.132**	50	172.991	11.027	30.508	**3**	56.984	6.054	32.115
		RBF	50	0.107	0.290	41.937	90	361.600	17.400	71.145	3	116.628	8.705	82.814
	Without COVID	ELM	3	0.084	0.242	26.932	35	472.051	19.277	65.402	30	118.146	9.505	69.580
		ESN	3	0.091	0.250	27.321	45	361.426	17.398	61.243	25	113.501	8.461	71.963
		MLP	5	0.072	0.214	23.736	3	229.299	12.624	32.513	**5**	**43.484**	**5.494**	**23.216**
		RBF	90	0.106	0.290	41.855	90	361.762	17.414	71.173	10	115.453	8.930	82.345
	Without COVID and Lockdown	ELM	55	0.226	0.389	45.342	25	445.110	18.727	58.367	35	140.325	9.701	72.964
		ESN	3	0.095	0.267	31.366	60	326.904	16.261	51.552	8	88.244	8.180	51.650
		MLP	5	0.096	0.237	24.660	5	268.293	12.734	30.227	12	69.210	5.750	24.045
		RBF	90	0.109	0.292	42.106	60	364.251	17.591	71.336	70	116.452	8.750	82.979

			NO$_2$				NO				O$_3$			
			NN	MSE	MAE	MAPE	NN	MSE	MAE	MAPE	NN	MSE	MAE	MAPE
Without Z-Score	All Inputs	ELM	3	570.143	18.949	26.896	5	5078.089	59.080	50.701	3	152.666	9.651	14.731
		ESN	3	523.303	17.204	27.192	12	15628.355	107.259	111.761	3	175.935	8.487	14.828
		MLP	70	608.078	19.198	19.419	**70**	**3433.167**	**42.272**	**27.680**	**3**	**99.301**	**8.259**	**11.462**
		RBF	5	886.859	25.285	36.021	5	8659.767	76.705	156.927	3	302.236	11.996	20.629
	Without COVID	ELM	3	510.554	19.691	24.813	3	49881.516	137.964	1172.231	3	276.657	13.781	18.821
		ESN	3	627.172	21.815	32.491	3	78881.981	219.920	827.994	15	586.099	20.913	30.830
		MLP	**55**	**353.000**	**16.116**	**18.310**	25	9192.320	42.764	66.788	70	123.546	8.233	13.090
		RBF	7	867.116	24.994	35.427	3	111554.876	285.136	2637.350	80	301.881	11.907	20.519
	Without COVID and Lockdown	ELM	3	749.904	24.518	33.485	3	6961.111	72.554	73.985	3	131.299	9.394	12.071
		ESN	15	1861.376	36.211	58.479	45	25439.828	123.837	229.898	3	269.781	13.052	16.959
		MLP	3	851.311	25.370	26.479	50	4811.999	53.290	37.489	90	101.570	6.857	11.121
		RBF	90	898.970	25.540	36.594	3	9205.445	81.435	160.595	90	301.796	11.914	20.527
With Z-Score	All Inputs	ELM	3	487.354	18.486	21.649	3	6057.239	63.555	91.520	3	136.731	9.546	15.309
		ESN	3	495.247	17.895	26.537	8	13938.590	98.401	127.912	7	238.876	13.117	18.446
		MLP	40	582.091	18.977	18.885	80	4080.494	49.610	28.741	17	113.758	8.885	12.352
		RBF	10	889.713	25.358	36.396	3	8805.067	77.825	158.019	3	302.235	11.985	20.620
	Without COVID	ELM	3	474.979	15.936	20.734	3	60013.692	214.782	1084.430	8	264.538	13.597	18.703
		ESN	3	842.937	25.159	36.858	3	80788.855	203.875	1247.237	5	241.888	14.196	18.513
		MLP	45	533.281	16.090	15.524	3	7461.860	40.342	65.189	90	127.865	9.106	14.463
		RBF	12	804.605	24.276	35.628	3	109705.490	283.427	2652.255	90	302.142	11.933	20.552
	Without COVID and Lockdown	ELM	3	695.472	18.534	27.748	3	5391.007	57.438	58.166	3	131.299	9.394	12.071
		ESN	60	1887.730	36.051	58.700	40	25912.029	124.420	240.393	3	347.065	15.199	19.339
		MLP	5	763.582	23.187	22.621	80	4334.745	49.248	33.712	90	134.022	8.179	12.276
		RBF	90	898.803	25.535	36.590	90	9225.294	78.847	160.696	90	300.184	11.808	20.385

NN: Number of neurons; MSE: Mean Square Error; MAE: Mean Absolute Error; MAPE: Mean Absolute Percentage Error; *With COVID means including the number of COVID-19 new cases and the partial lockdown.

Table A2
Computational results for D. Pedro II Station

			CO				PM$_{10}$				PM$_{2.5}$			
			NN	MSE	MAE	MAPE	NN	MSE	MAE	MAPE	NN	MSE	MAE	MAPE
Without *Z-Score*	All Inputs	ELM	5	0.145	0.274	46.448	3	201.221	11.965	49.041	3	51.303	5.935	39.177
		ESN	3	0.236	0.446	175.795	3	71.156	7.847	32.640	3	57.354	6.088	69.635
		MLP	3	0.133	0.257	45.423	5	**62.832**	**6.936**	**28.881**	3	18.305	3.323	19.678
		RBF	3	0.206	0.420	175.738	90	232.000	13.800	67.802	90	61.650	6.700	71.874
	Without COVID	ELM	3	0.088	0.220	60.253	3	167.635	10.469	34.639	3	67.776	6.738	42.641
		ESN	12	0.303	0.467	206.963	15	417.394	17.723	93.584	5	88.044	8.547	79.455
		MLP	45	0.101	0.242	42.666	15	73.638	7.079	26.922	60	18.683	3.579	23.942
		RBF	3	0.204	0.419	174.983	90	232.206	13.805	67.810	90	61.697	6.702	71.883
	Without COVID and Lockdown	ELM	3	0.119	0.251	59.499	3	378.428	15.714	44.049	3	66.176	6.592	41.157
		ESN	7	0.313	0.478	185.849	3	252.998	13.814	68.271	3	82.455	7.507	75.413
		MLP	45	0.111	0.276	55.548	40	79.912	8.113	33.120	40	27.414	4.675	25.319
		RBF	5	0.198	0.414	172.176	94	232.421	13.810	67.819	90	61.713	6.703	71.886
With *Z-Score*	All Inputs	ELM	3	0.096	0.227	39.350	3	127.320	9.337	33.624	3	33.077	5.200	48.258
		ESN	7	0.340	0.511	201.290	3	218.389	12.568	60.732	3	54.302	6.176	67.292
		MLP	**3**	**0.069**	**0.200**	**48.480**	80	76.843	7.220	24.859	**3**	**15.806**	**3.582**	**28.000**
		RBF	5	0.205	0.420	175.627	90	232.000	13.800	67.802	60	61.650	6.700	71.874
	Without COVID	ELM	5	0.123	0.268	67.011	3	101.629	8.641	35.393	3	54.781	6.227	42.818
		ESN	20	0.392	0.543	239.621	3	294.932	14.778	73.650	3	88.592	7.841	62.774
		MLP	25	0.117	0.240	48.976	10	100.519	7.814	30.358	80	18.872	3.395	22.804
		RBF	3	0.203	0.419	174.831	90	232.206	13.805	67.810	90	61.697	6.702	71.883
	Without COVID and Lockdown	ELM	3	0.106	0.281	47.589	3	280.543	13.438	54.251	3	42.747	5.443	38.441
		ESN	15	0.390	0.550	239.796	3	325.950	14.608	66.276	5	120.188	8.986	96.500
		MLP	12	0.101	0.269	53.239	80	79.421	8.156	33.803	12	26.396	4.350	28.352
		RBF	3	0.199	0.416	171.079	90	232.429	13.810	67.820	90	61.713	6.703	71.886

			NO$_2$				NO				O$_3$			
			NN	MSE	MAE	MAPE	NN	MSE	MAE	MAPE	NN	MSE	MAE	MAPE
Without *Z-Score*	All Inputs	ELM	5	785.090	20.353	30.175	10	4839.146	50.450	153.333	7	467.375	15.322	34.491
		ESN	5	907.308	24.263	40.671	10	4772.463	58.378	373.840	3	353.385	15.163	32.252
		MLP	70	557.778	17.589	23.740	**50**	**2657.192**	**38.072**	**81.015**	7	138.893	9.422	16.985
		RBF	5	854.313	25.362	51.069	5	5416.426	68.009	486.657	17	454.931	17.020	36.846
	Without COVID	ELM	3	445.282	17.293	23.027	7	4340.598	57.558	348.301	5	63.055	5.997	12.454
		ESN	3	822.075	25.260	52.416	3	5996.855	71.571	445.188	3	260.122	12.669	26.255
		MLP	35	464.065	17.072	21.113	8	3924.373	45.396	86.404	45	120.824	9.143	16.909
		RBF	5	854.784	25.517	51.092	5	5461.894	68.337	488.802	3	391.845	15.011	33.241
	Without COVID and Lockdown	ELM	7	1064.275	27.726	57.589	3	3991.357	54.068	113.379	3	137.191	9.229	17.298
		ESN	10	1555.614	31.140	75.076	15	8592.139	80.821	675.729	40	1214.000	29.877	59.143
		MLP	40	295.496	14.269	22.207	12	4320.338	48.815	91.635	3	206.566	12.420	21.391
		RBF	90	868.487	25.612	51.959	90	5472.401	68.400	490.933	3	358.350	12.872	29.566
With *Z-Score*	All Inputs	ELM	3	663.132	16.812	19.980	7	4307.805	50.687	159.321	3	115.769	9.348	18.562
		ESN	3	1070.911	26.303	35.021	30	5849.480	67.123	420.655	3	489.524	18.494	37.389
		MLP	60	493.319	18.015	23.994	35	3274.156	46.066	84.661	**40**	**86.199**	**7.354**	**13.290**
		RBF	7	864.579	25.509	51.690	3	5402.146	67.809	477.883	20	456.534	17.058	36.916
	Without COVID	ELM	5	394.529	16.522	29.060	5	3768.178	54.428	120.683	3	43.501	5.673	10.074
		ESN	3	902.434	26.099	51.690	3	5501.005	68.838	471.550	3	260.471	11.801	25.214
		MLP	**20**	**228.207**	**12.518**	**20.777**	7	3911.060	47.170	76.890	5	89.321	7.703	14.095
		RBF	12	859.824	25.425	52.147	3	5401.730	67.974	478.234	3	391.500	14.998	33.216
	Without COVID and Lockdown	ELM	3	782.711	24.452	39.246	3	5041.661	61.826	202.719	3	107.910	7.838	16.488
		ESN	40	1871.582	36.537	83.638	12	8067.633	80.195	594.801	3	389.735	14.920	28.355
		MLP	55	346.735	16.076	26.940	7	4490.207	51.747	87.543	3	161.224	10.402	19.405
		RBF	90	868.484	25.612	51.959	40	5471.100	68.391	490.941	5	369.729	13.681	31.046

NN: Number of neurons; MSE: Mean Square Error; MAE: Mean Absolute Error; MAPE: Mean Absolute Percentage Error; *With COVID means including the variables number of COVID-19 new cases and the partial lockdown.
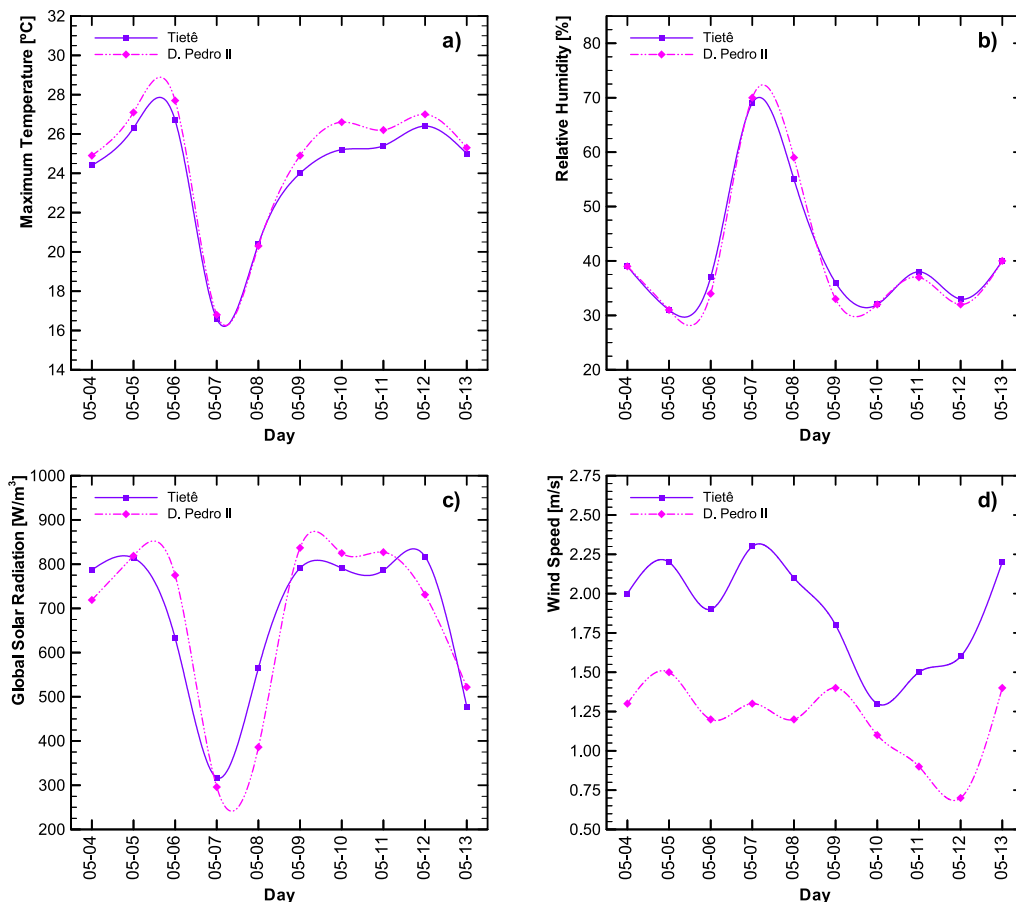
Fig. A3. Meteorological variables raw data for the test set.

References

Andrade, M. de F., Kumar, P., de Freitas, E.D., Ynoue, R.Y., Martins, J., Martins, L.D., Nogueira, T., Perez-Martinez, P., de Miranda, R.M., Albuquerque, T., Gonçalves, F.L.T., Oyama, B., Zhang, Y., 2017. Air quality in the megacity of São Paulo: evolution over the last 30 years and future perspectives. Atmos. Environ. 159, 66–82. https://doi.org/10.1016/j.atmosenv.2017.03.051.

Araujo, L.N., Belotti, J.T., Antonini Alves, T., Tadano, Y. de S., Siqueira, H., 2020. Ensemble method based on Artificial Neural Networks to estimate air pollution health risks. Environ. Model. Software 123, 104567. https://doi.org/10.1016/j.envsoft.2019.104567.

CETESB, 2020. Environmental Companyof São Paulo State (in Portuguese: Companhia Ambiental do Estado de São Paulo). http://cetesb.sp.gov.br/ar/qualar/. (Accessed 15 May 2020).

Chauhan, A., Singh, R.P., 2020. Decline in PM$_{2.5}$ concentrations over major cities around the world associated with COVID-19. Environ. Res. 187, 109634. https://doi.org/10.1016/j.envres.2020.109634.

CNBC, 2020. South America Is a 'new Epicenter' of the Coronavirus Pandemic. WHO says. https://www.cnbc.com/2020/05/22/south-america-is-a-new-epicenter-of-the-coronavirus-pandemic-who-says.html. (Accessed 25 May 2020).

Dantas, G., Siciliano, B., França, B.B., da Silva, C.M., Arbilla, G., 2020. The impact of COVID-19 partial lockdown on the air quality of the city of Rio de Janeiro, Brazil. Sci. Total Environ. 729, 139085. https://doi.org/10.1016/j.scitotenv.2020.139085.

de Castro, L.N., 2007. Fundamentals of natural computing: an overview. Phys. Life Rev. 4 (1), 1–36. https://doi.org/10.1016/j.plrev.2006.10.002.

de Oliveira, G., Chen, J.M., Stark, S.C., Berenguer, E., Moutinho, P., Artaxo, P., Anderson, L.O., Aragão, L.E.O.C., 2020. Smoke pollution's impacts in Amazonia. Science 369 (6504), 634–635. https://doi.org/10.1126/science.abd5942.

dos Santos, E.P., Von Zuben, F.J., 1999. Improved second-order training algorithms for globally and partially recurrent neural networks. In: Proceedings of the International Joint Conference on Neural Networks. https://doi.org/10.1109/ijcnn.1999.832591.

Dutheil, F., Baker, J.S., Navel, V., 2020. COVID-19 as a factor influencing air pollution? Environ. Pollut. 263, Par A, 114466. https://doi.org/10.1016/j.envpol.2020.114466.

Figueiredo, E., Macedo, M., Siqueira, H.V., Santana, C.J., Gokhale, A., Bastos-Filho, C.J.A., 2019. Swarm intelligence for clustering — a systematic review with new perspectives on data mining. Eng. Appl. Artif. Intell. 82, 313–329. https://doi.org/10.1016/j.engappai.2019.04.007.

Gentner, D.R., Harley, R.A., Miller, A.M., Goldstein, A.H., 2009. Diurnal and seasonal variability of gasoline-related volatile organic compound emissions in Riverside, California. Environ. Sci. Technol. 43 (12), 4247–4252. https://doi.org/10.1021/es9006228.

Guardani, R., Nascimento, C.A.O., Guardani, M.L.G., Martins, M.H.R.B., Romano, J., 1999. Study of atmospheric ozone formation by means of a neural network-based model. J. Air Waste Manag. Assoc. 49 (3), 316–323. https://doi.org/10.1080/10473289.1999.10463806.

Guardian, The, 2020. Brazil Scales Back Environmental Enforcement amid Coronavirus Outbreak. https://www.theguardian.com/world/2020/mar/27/brazil-scales-back-environmental-enforcement-coronavirus-outbreak-deforestation. (Accessed 22 May 2020).

IBGE, 2020. The Brazilian Institute of Geography and Statistics (in Portuguese: Instituto Brasileiro de Geografia e Estatística). (Accessed 15 May 2020).

Harley, R.A., Marr, L.C., Lehner, J.K., Giddings, S.N., 2005. Changes in motor vehicle emissions on diurnal to decadal time scales and effects on atmospheric composition. Environ. Sci. Technol. 39 (14), 5356–5362. https://doi.org/10.1021/es048172+.

Haykin, S., 2008. Neural Networks and Learning Machines. Pearson Prentice Hall New Jersey USA 936 pLinks https://doi.org/978-0131471399.

Hong, C., Zhang, Q., Zhang, Y., Davis, S.J., Tong, D., Zheng, Y., Liu, Z., Guan, D., He, K., Schellnhuber, H.J., 2019. Impacts of climate change on future air quality and human health in China. Proc. Natl. Acad. Sci. U. S. A 116 (35), 17193–17200. https://doi.org/10.1073/pnas.1812881116.

Huang, G. Bin, Zhu, Q.Y., Siew, C.K., 2006. Extreme Learning Machine: Theory and Applications. Neurocomputing. https://doi.org/10.1016/j.neucom.2005.12.126.

Huang, Gao, Huang, Guang Bin, Song, S., You, K., 2015. Trends in Extreme Learning Machines: A Review. Neural Networks. https://doi.org/10.1016/j.neunet.2014.10.001.

Jaeger, H., 2001. The "echo state" approach to analysing and training recurrent neural networks. GMD Rep 148 (34), 13.

Jaeger, H., 2002. Short Term Memory in Echo State Networks. GMD Report 152.

Kachba, Y., de Genaro Chiroli, D.M., Belotti, J.T., Antonini Alves, T., de Souza Tadano, Y., Siqueira, H., 2020. Artificial neural networks to estimate the influence of vehicular emission variables on morbidity and mortality in the largest metropolis in South America. Sustain. Times 12 (7), 2621. https://doi.org/10.3390/su12072621.

Kassomenos, P., Petrakis, M., Sarigiannis, D., Gotti, A., Karakitsios, S., 2011. Identifying the contribution of physical and chemical stressors to the daily number of hospital admissions implementing an artificial neural network model. Air Qual. Atmos. Heal. 4, 263–272. https://doi.org/10.1007/s11869-011-0139-2.

Le, T., Wang, Y., Liu, L., Yang, J., Yung, Y.L., Li, G., Seinfeld, J.H., 2020. Unexpected air pollution with marked emission reductions during the COVID-19 outbreak in China. Science 369 (6504), 702–706. https://doi.org/10.1126/science.abb7431.

Li, K., Jacob, D.J., Liao, H., Shen, L., Zhang, Q., Bates, K.H., 2019. Anthropogenic drivers of 2013−2017 trends in summer surface ozone in China. Proc. Natl. Acad. Sci. U. S. A 116 (2), 422−427. https://doi.org/10.1073/pnas.1812168116.

Li, L., Li, Q., Huang, L., Wang, Q., Zhu, A., Xu, J., Liu, Ziyi, Li, H., Shi, L., Li, R., Azari, M., Wang, Y., Zhang, X., Liu, Zhiqiang, Zhu, Y., Zhang, K., Xue, S., Ooi, M.C.G., Zhang, D., Chan, A., 2020. Air quality changes during the COVID-19 lockdown over the Yangtze River Delta Region: an insight into the impact of human activity pattern changes on air pollution variation. Sci. Total Environ. 732, 139282. https://doi.org/10.1016/j.scitotenv.2020.139282.

Marr, L.C., Harley, R.A., 2002. Spectral analysis of weekday-weekend differences in ambient ozone, nitrogen oxide, and non-methane hydrocarbon time series in California. Atmos. Environ. 36 (14), 2327−2335. https://doi.org/10.1016/S1352-2310(02)00188-7.

Martins, L.D., Andrade, M.D.F., 2008. Ozone formation potentials of volatile organic compounds and ozone sensitivity to their emission in the megacity of São Paulo, Brazil. Water. Air. Soil Pollut 195, 201−213. https://doi.org/10.1007/s11270-008-9740-x.

Muhammad, S., Long, X., Salman, M., 2020. COVID-19 pandemic and environmental pollution: a blessing in disguise? Sci. Total Environ. 728, 138820. https://doi.org/10.1016/j.scitotenv.2020.138820.

Nakada, L.Y.K., Urban, R.C., 2020. COVID-19 pandemic: impacts on the air quality during the partial lockdown in São Paulo state. Brazil. Sci. Total Environ. 730, 139087. https://doi.org/10.1016/j.scitotenv.2020.139087.

Polezer, G., Tadano, Y.S., Siqueira, H.V., Godoi, A.F.L., Yamamoto, C.I., de André, P.A., Pauliquevis, T., Andrade, M. de F., Oliveira, A., Saldiva, P.H.N., Taylor, P.E., Godoi, R.H.M., 2018. Assessing the impact of PM2.5 on respiratory disease using artificial neural networks. Environ. Pollut. 235, 394−403. https://doi.org/10.1016/j.envpol.2017.12.111.

Rodríguez-Urrego, D., Rodríguez-Urrego, L., 2020. Air quality during the COVID-19: PM2.5 analysis in the 50 most polluted capital cities in the world. Environ. Pollut. 266 - Part 1, 115042. https://doi.org/10.1016/j.envpol.2020.115042.

SEADE, 2020. Statistical Portal of São Paulo State (in Portuguese: Portal de Estatísticas do Estado de São Paulo). https://www.seade.gov.br/coronavirus/. (Accessed 12 June 2020).

Seinfeld, J.H., Pandis, S.N., 2016. Atmospheric Chemistry and Physics: from Air Pollution to Climate Change. John Wiley & Sons.

Sharma, S., Zhang, M., Anshika, Gao, J., Zhang, H., Kota, S.H., 2020. Effect of restricted emissions during COVID-19 on air quality in India. Sci. Total Environ. 728, 138878. https://doi.org/10.1016/j.scitotenv.2020.138878.

Shehzad, K., Sarfraz, M., Shah, S.G.M., 2020. The impact of COVID-19 as a necessary evil on air pollution in India during the lockdown. Environ. Pollut. 266 - Part 1, 115080. https://doi.org/10.1016/j.envpol.2020.115080.

Sicard, P., De Marco, A., Agathokleous, E., Feng, Z., Xu, X., Paoletti, E., Rodriguez, J.J.D.,

Calatayud, V., 2020. Amplified ozone pollution in cities during the COVID-19 lockdown. Sci. Total Environ. 735, 139542. https://doi.org/10.1016/j.scitotenv.2020.139542.

Siciliano, B., Dantas, G., da Silva, C.M., Arbilla, G., 2020. Increased ozone levels during the COVID-19 lockdown: analysis for the city of Rio de Janeiro, Brazil. Sci. Total Environ. 737, 139765. https://doi.org/10.1016/j.scitotenv.2020.139765.

Sillman, S., 1999. The relation between ozone, NO(x) and hydrocarbons in urban and polluted rural environments. Atmos. Environ. 33 (12), 1821−1845. https://doi.org/10.1016/S1352-2310(98)00345-8.

Sillman, S., 2003. Tropospheric ozone and photochemical smog. In: Treatise on Geochemistry, 9. Elsevier Science, pp. 407−431.

Siqueira, H., Luna, I., 2019. Performance comparison of feedforward neural networks applied to streamflow series forecasting. Math. Eng. Sci. Aerosp. 10 (1), 41−53.

Siqueira, H., Boccato, L., Attux, R., Lyra, C., 2012a. Echo state networks and extreme learning machines: a comparative study on seasonal streamflow series prediction. In: Lecture Notes in Computer Science (Including Subseries Lecture Notes in Artificial Intelligence and Lecture Notes in Bioinformatics). https://doi.org/10.1007/978-3-642-34481-7_60.

Siqueira, H., Boccato, L., Attux, R., Lyra, C., 2012b. Echo state networks for seasonal stremflow series forecasting. In: Lecture Notes in Computer Science (Including Subseries Lecture Notes in Artificial Intelligence and Lecture Notes in Bioinformatics). https://doi.org/10.1007/978-3-642-32639-4_28.

Siqueira, H., Boccato, L., Attux, R., Lyra, C., 2014. Unorganized machines for seasonal streamflow series forecasting. Int. J. Neural Syst. 24 (3), 14300009. https://doi.org/10.1142/S0129065714300095.

Siqueira, H., Boccato, L., Luna, I., Attux, R., Lyra, C., 2018. Performance analysis of unorganized machines in streamflow forecasting of Brazilian plants. Appl. Soft Comput. J. 68, 494−506. https://doi.org/10.1016/j.asoc.2018.04.007.

Siqueira, H., Macedo, M., Tadano, Y.S., Antonini Alves, T., Stevan Jr., S.L., Oliveira, D.S., Marinho, M.H.N., Neto, P.S.G., de, M., Oliveira, Joao, F.L., deLuna, I., Filho, M., de, A.L., Sarubbo, L.A., Converti, A., 2020. Selection of temporal lags for predicting riverflow series from hydroelectric plants using variable selection methods. Energies 13 (16), 4236. https://doi.org/10.3390/en13164236.

Stedman, D.H., 2004. Photochemical ozone formation, simplified. Environ. Chem. 1 (2), 65−66. https://doi.org/10.1071/EN04032.

Tadano, Yara S., Siqueira, Hugo, Antonini Alves, Thiago, 2016. Unorganized machines to predict hospital admissions for respiratory diseases. 2016 IEEE Latin Am. Conf. Comput. Intell. (LA-CCI) 1, 1−6. https://doi.org/10.1109/LA-CCI.2016.7885699.

The Lancet, 2020. COVID-19 in Brazil: "so what?" Lancet. https://doi.org/10.1016/S0140-6736(20)31095-3.

Tobías, A., Carnerero, C., Reche, C., Massagué, J., Via, M., Minguillón, M.C., Alastuey, A., Querol, X., 2020. Changes in air quality during the lockdown in Barcelona (Spain) one month into the SARS-CoV-2 epidemic. Sci. Total Environ. 726, 138540. https://doi.org/10.1016/j.scitotenv.2020.138540.

Wilder-Smith, A, Freedman, D.O., 2020. Isolation, quarantine, social distancing and community containment: Pivotal role for old-style public health measures in the Novel Coronavirus (2019-nCoV) outbreak. J. Travel Med. 27 (2), 1−4. https://doi.org/10.1093/jtm/taaa020.

Wu, X., Nethery, R.C., Sabath, B.M., Braun, D., Dominici, F., 2020. Exposure to Air Pollution and COVID-19 Mortality in the United States. medRxiv. https://doi.org/10.1101/2020.04.05.20054502.

Zambrano-Monserrate, M.A., Ruano, M.A., Sanchez-Alcalde, L., 2020. Indirect effects of COVID-19 on the environment. Sci. Total Environ. 728, 138813. https://doi.org/10.1016/j.scitotenv.2020.138813.